



Effects of rapid thermal annealing on two-dimensional delocalized electronic states of the epitaxial N δ -doped layer in GaAs

Ogawa, Yasuhiro
Harada, Yukihiro
Baba, Takeshi
Kaizu, Toshiyuki
Kita, Takashi

(Citation)

Applied Physics Letters, 108(11):111905-111905

(Issue Date)

2016-03-14

(Resource Type)

journal article

(Version)

Version of Record

(Rights)

©2016 AIP Publishing. This article may be downloaded for personal use only. Any other use requires prior permission of the author and AIP Publishing. The following article appeared in Applied Physics Letters 108(11), 111905 and may be found at <http://dx.doi.org/10.1063/1.4944055>

(URL)

<https://hdl.handle.net/20.500.14094/90003347>



Effects of rapid thermal annealing on two-dimensional delocalized electronic states of the epitaxial N δ -doped layer in GaAs

Yasuhiro Ogawa, Yukihiro Harada, Takeshi Baba, Toshiyuki Kaizu, and Takashi Kita

Citation: [Applied Physics Letters](#) **108**, 111905 (2016); doi: 10.1063/1.4944055

View online: <http://dx.doi.org/10.1063/1.4944055>

View Table of Contents: <http://scitation.aip.org/content/aip/journal/apl/108/11?ver=pdfcov>

Published by the [AIP Publishing](#)

Articles you may be interested in

[Epitaxial two-dimensional nitrogen atomic sheet in GaAs](#)

Appl. Phys. Lett. **104**, 041907 (2014); 10.1063/1.4863442

[A quantitative model for the blueshift induced by rapid thermal annealing in GaNAs/GaAs triple quantum wells](#)

J. Appl. Phys. **96**, 2586 (2004); 10.1063/1.1776638

[Rapid thermal annealing effects on step-graded InAlAs buffer layer and In 0.52 Al 0.48 As/In 0.53 Ga 0.47 As metamorphic high electron mobility transistor structures on GaAs substrates](#)

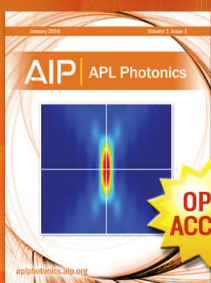
J. Appl. Phys. **91**, 2429 (2002); 10.1063/1.1433174

[Electronic and isochronal annealing properties of electron traps in rapid thermally annealed SiO₂-capped n-type GaAs epitaxial layers](#)

J. Appl. Phys. **88**, 5255 (2000); 10.1063/1.1314907

[Mechanism for rapid thermal annealing improvements in undoped GaN_xAs_{1-x}/GaAs structures grown by molecular beam epitaxy](#)

Appl. Phys. Lett. **77**, 2325 (2000); 10.1063/1.1315632



Launching in 2016!
The future of applied photonics research is here

AIP | APL
Photonics

Effects of rapid thermal annealing on two-dimensional delocalized electronic states of the epitaxial N δ -doped layer in GaAs

Yasuhiro Ogawa, Yukihiro Harada, Takeshi Baba, Toshiyuki Kaizu, and Takashi Kita
 Department of Electrical and Electronic Engineering, Graduate School of Engineering, Kobe University,
 1-1 Rokkodai, Nada, Kobe 657-8501, Japan

(Received 4 December 2015; accepted 3 March 2016; published online 18 March 2016)

We have conducted rapid thermal annealing (RTA) for improving the two-dimensional (2D) arrangement of electronic states in the epitaxial nitrogen (N) δ -doped layer in GaAs. RTA rearranged the N-pair configurations in the GaAs (001) plane and reduced the number of non-radiative recombination centers. Furthermore, a Landau shift, representing the 2D delocalized electronic states in the (001) plane, was observed at around zero magnetic field intensity in the Faraday configuration. © 2016 AIP Publishing LLC. [<http://dx.doi.org/10.1063/1.4944055>]

Recent progress in electronic and optoelectronic devices results from the precise control of the electronic states in semiconductors via the charge carrier confinement in the heterostructures. Zero-dimensional self-assembled quantum dots (QDs) have been strenuously studied for the realization of the low-threshold lasers, high-speed semiconductor optical amplifiers, single- and entangled-photon sources, and non-volatile fast memory devices.¹ On the other hand, the electronic coupling between the vertical and lateral QDs modifies their electronic states^{2–4} and changes the carrier confinement dimension.^{5,6} These artificial controls of electronic states open the functionality to make high-performance devices. However, the inhomogeneous distribution of the size and shape of the QDs prevents forming the coherently coupled electronic states in the growth plane. Besides, single impurity centers or dopants in semiconductors have been regarded as qubits for quantum computing and nonclassical light sources for quantum information processing as well as QDs.⁷ The electronic state of the localized impurity level is uniquely determined by a combination of the host matrix and the impurity centers. Therefore, the coherently coupled electronic states among the impurities are expected for the highly impurity-doped semiconductors in the atomically controlled way.

Recently, we have successfully grown an epitaxial nitrogen (N) δ -doped layer embedded in GaAs using the site-controlled N δ -doping technique that we developed.⁸ N δ -doping is an effective technique allowing control of the N-pair configuration^{9–11} and engineering of the band structure.^{12,13} In the impurity limit, N pair centers in GaAs act as isoelectronic traps below the conduction-band edge because of a strong electronegativity of N atoms.^{9,14–16} The electronic state of the localized impurity level is uniquely determined by the N pair structure in GaAs, thereby electronic coupling among high-density N pair centers enables to form a quasi epitaxial sheet. By increasing the N δ -doping density, we observed a change in the electronic states in the N δ -doped GaAs from the isolated impurity centers to the delocalized impurity band at 1.49 eV according to the photoluminescence (PL) spectroscopy.⁸ The emission line at 1.49 eV was attributed to the fourth-nearest-neighbor N pairs in the growth plane.⁸ We observed a Landau shift of the 1.49 eV

band resulting from the delocalized electronic states in the Faraday configuration for the epitaxial N δ -doped layer, indicating a high carrier mobility supra $10\,000\text{ cm}^2/\text{V s}$ in the embedded layer comprised sp^3 -hybridized bonds.⁸ The epitaxial N δ -doped layer embedded in GaAs presents a promising advantage for practical applications such as field-effect-transistor channels. However, the Landau shift has been observed only above 3.5 T, suggesting a contribution the localized levels below the delocalized impurity band edge.⁸ It is well known that rapid thermal annealing (RTA) dramatically improves the crystal quality of bulk GaNAs¹⁷ and GaInNAs single quantum wells (SQWs)¹⁸ by rearranging the N atoms. In this study, we conducted RTA to prompt the rearrangement of N atoms in the GaAs (001) plane and studied the effects of the RTA on the two-dimensional (2D) properties.

All samples were grown by using molecular beam epitaxy (MBE) on a semi-insulating GaAs (001) substrate. Before N δ -doping, a 400-nm-thick GaAs buffer layer, a 300-nm-thick $\text{Al}_{0.3}\text{Ga}_{0.7}\text{As}$ layer, and a 50-nm-thick GaAs layer were grown. N δ -doping was performed on an atomically flat $(2 \times 4)\beta_2$ surface with a nitridation duration of 2000 s by using active atomic N species created using a radio-frequency plasma source from an ultrapure N_2 gas. After a 120-s-long growth interruption, 50-nm-thick GaAs, 100-nm-thick $\text{Al}_{0.3}\text{Ga}_{0.7}\text{As}$, and 10-nm-thick GaAs capping layers were grown. All of the layers were grown at 550°C , with the As_2 flux of $1.3 \times 10^{-3}\text{ Pa}$. According to secondary ion-microprobe mass spectrometry, the N sheet density was approximately $4.6 \times 10^4\text{ }\mu\text{m}^{-2}$. The N atoms distribute along the growth direction with a full-width at half-maximum of approximately 8 monolayers with a standard deviation of approximately 3 monolayers, according to the cross-sectional scanning tunneling microscope (XSTM) images.¹⁹ After removing the wafer from the MBE chamber, the sample was annealed at 650 and 850°C for 60 s, under N ambient condition. The sample was covered with a GaAs substrate to prevent As desorption during the annealing process.^{20,21}

PL measurements were performed using a continuous-wave laser beam ($\lambda = 484\text{ nm}$). The samples were mounted in a closed-cycle cryostat for the PL measurements and in a

superconducting-magnet system cooled by a He gas flow for the magneto-PL measurements. The PL signal was dispersed by a 55-cm single monochromator and was detected by using a liquid-N₂-cooled Si charge-coupled device array. Time-resolved PL measurements were performed using a mode-locked Ti:sapphire pulse laser ($\lambda = 750$ nm, pulse duration: ~ 140 fs, repetition frequency: 4 MHz), and the PL signal was detected by a streak camera system with a temporal resolution of 50 ps. A magnetic field was applied in the [001] direction in the Faraday configuration.

Figure 1 shows typical PL spectra for the epitaxial N δ -doped layer at 3.3 K. The black, red, and blue spectra are for the as-grown sample, the sample annealed at 650 °C, and the sample annealed at 850 °C, respectively. The green spectrum was obtained for the as-grown reference sample with the nitridation duration of 20 s. The excitation power was 2.5 W/cm². We confirmed that the PL intensities did not saturate for this excitation power. The PL peak at 1.444 eV is attributed to the excitons bound to the first-nearest-neighbor N pairs in the (001) plane.¹⁰ The broad PL peak in the 1.47–1.49 eV band results from the interaction between the two types of N pairs attributed to the bound exciton lines at 1.479 and 1.493 eV in the reference sample. The line at 1.493 eV is attributed to the excitons bound to the fourth-nearest-neighbor N pairs in the (001) plane.¹⁰ On the other hand, the line at 1.479 eV is attributed to the excitons bound to other N pairs in the (001) plane,¹⁴ which was not observed for the samples for which N δ -doping was performed on the $(2 \times 4)\alpha$ surface.¹¹ The broad energy peak in the 1.47–1.49 eV band exhibits a blueshift of 18 meV induced by the RTA. A similar RTA-induced blueshift was reported for GaNAs^{17,21} and GaInNAs bulk crystals,¹⁸ and was interpreted as a rearrangement of N atoms into a homogeneous atomic distribution.^{17,22} The peak intensity at 1.444 eV decreases with RTA. On the other hand, the peak intensity at

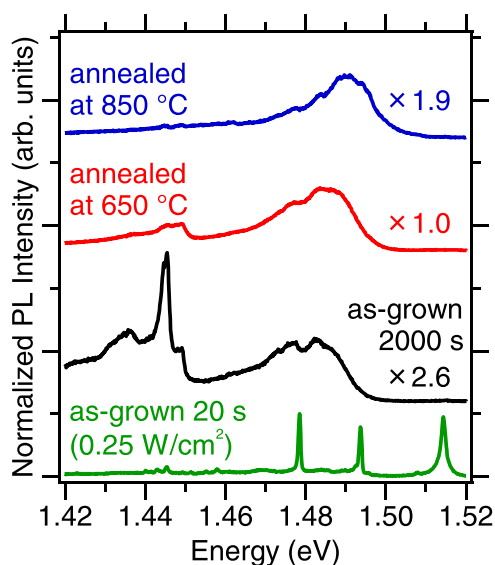


FIG. 1. Typical PL spectra for the epitaxial N δ -doped layer at 3.3 K. The black, red, and blue spectra are for the as-grown sample, the sample annealed at 650 °C, and the sample annealed at 850 °C, respectively. The excitation power was 2.5 W/cm². PL spectra were normalized at the 1.47–1.49 eV band. The green spectrum is for an as-grown reference sample with a nitridation duration of 20 s. The excitation power was 0.25 W/cm².

1.47–1.49 eV increases by 2.6 times for the sample annealed at 650 °C, and by 1.3 times for the sample annealed at 850 °C. The reduction in the peak intensity at 1.47–1.49 eV for the sample annealed at 850 °C is attributed to the diffusion of N atoms out of the sample.^{17,21} In Fig. 1, the other energy peaks were not newly emerging and only the PL peak intensities at 1.444 eV and 1.47–1.49 eV changed. This suggests that the RTA process induces a rearrangement of N atoms belonging to the first-nearest-neighbor N pairs to the fourth-nearest-neighbor N pairs. Because the sample annealed at 650 °C exhibited a relatively stronger increase in the peak intensity at 1.47–1.49 eV, we proceeded to compare the detailed properties of the as-grown sample and that annealed at 650 °C.

The increase in the peak intensity at 1.47–1.49 eV can also be caused by a reduction in the number of non-radiative recombination centers. N atoms in GaAs tend to form non-radiative recombination centers originating from, for example, two atoms at a single As site, such as NN_{As} and AsN_{As}.²³ Actually, in the case of the bulk mixed crystal semiconductors such as GaNAs and GaInNAs, the non-radiative recombination centers can be eliminated by RTA owing to a rearrangement of N atoms.^{23,24} To investigate the reduction in the number of non-radiative recombination centers, we performed temperature-dependent PL measurements. Figures 2(a) and 2(b) show the temperature dependences of the PL spectra for the as-grown sample excited at 250 W/cm² and the sample that was annealed at 650 °C and excited at 25 W/cm². Here, we chose different maximal excitation power values that did not cause saturations of the corresponding peak intensities. The PL spectra were normalized by the peak intensities from Figs. 2(a) and 2(b). The PL intensity of the broad band at 1.47–1.49 eV decreased with increasing the temperature. Figure 2(c) shows the Arrhenius plot of the PL intensity for the 1.47–1.49 eV band. The estimated thermal quenching activation energies (E_a) were 11.1 ± 0.4 and 24.4 ± 3.6 meV for the as-grown sample and that annealed at 650 °C, respectively. The increase in the activation energy indicates a reduction in the number of

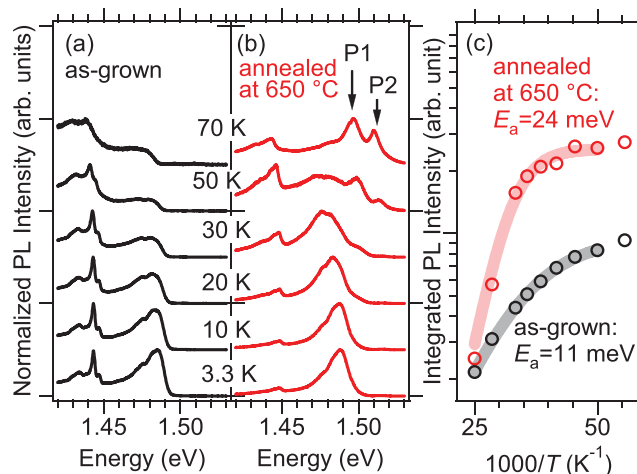


FIG. 2. Temperature dependence of the PL spectra for (a) the as-grown sample and (b) the sample annealed at 650 °C. The excitation powers were 250 and 25 W/cm², respectively. PL spectra were normalized by the peak intensities. (c) Arrhenius plot of the PL intensity for the 1.47–1.49 eV band. The solid lines show the fitting curves.

non-radiative recombination centers by the RTA. A similar increase in the activation energy, which was caused by diminishing the compositional fluctuation of N and In atoms, has been reported for GaInNAs SQWs.²¹

On the other hand, for the sample annealed at 650 °C, the two peaks of P1 and P2 appeared above 30 K. According to the results of our previous work, P1 and P2 can be attributed to the biexciton at 1.493 eV with a negative binding energy and the GaAs free exciton, respectively.²⁵ These peaks also appeared for the excitation power above $\sim 125 \text{ W/cm}^2$ at 3.3 K, and the peak intensity of P1 exhibited a quadratic dependence on that of the 1.493 eV line. The appearance of P1 and P2 above 30 K suggests a thermally activated bound-exciton dissociation with a reduced non-radiative recombination process.

In order to clarify the dimensionality of the electronic states in the epitaxial N δ -doped layer, we studied the temperature-dependent radiative lifetime. Figure 3(a) shows the PL decay profiles for the 1.47–1.49 eV band of the as-grown sample and that annealed at 650 °C at 3.7 K. Both the PL-decay profiles exhibit two decay components; the fast and slow components result from the delocalized and localized electronic states, respectively. The ratio of the fast and slow components, $I_{\text{fast}}/I_{\text{slow}}$, for the sample annealed at 650 °C was approximately two times stronger than that for the as-grown sample, resulting from the enhancement of delocalization degree due to the rearrangement of N atoms as discussed in Fig. 1. The decay times of the fast (slow) component of the as-grown sample and that annealed at 650 °C were 0.35 (7.2) and 0.45 (2.8) ns, respectively. These decay times were faster than the decay time of 11 ns for the localized excitons bound to the fourth-nearest-neighbor N pairs in the impurity limit.¹¹ In general, decay time τ includes both the radiative lifetime τ_r and the non-radiative lifetime τ_{nr} . To obtain the τ_r , we took into account the temperature-dependent PL intensity $I_{\text{PL}}(T)$ by assuming that the temperature-dependent radiative yield $\eta(T) = \tau_r^{-1}/(\tau_r^{-1} + \tau_{\text{nr}}^{-1})$

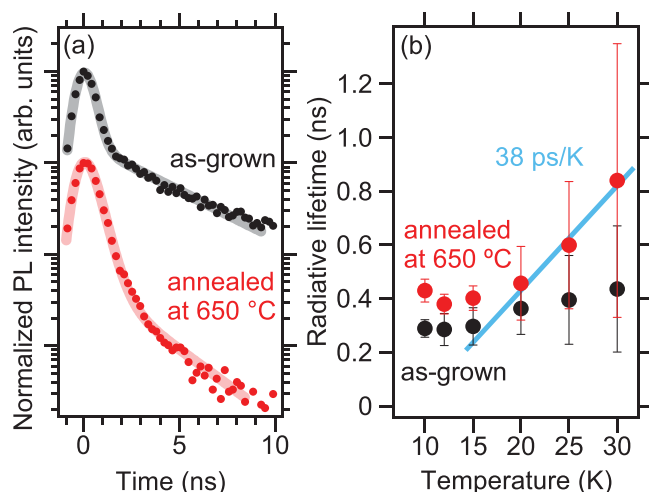


FIG. 3. (a) PL decay profiles for the 1.47–1.49 eV band of the as-grown sample and that annealed at 650 °C at 3.7 K. The excitation density was 90 nJ/cm². The solid lines show the fitting results. (b) Temperature dependence of the radiative lifetime of the fast component for the as-grown samples and that annealed at 650 °C. The solid line shows the fitting result at above 20 K for the sample annealed at 650 °C.

corresponds to the $I_{\text{PL}}(T)$.²⁶ The temperature-dependent radiative lifetime $\tau_r(T)$ is given by $\tau_r(T) = \tau_r(0)/\eta(T)$ with an assumption of negligible non-radiative process at $T = 0 \text{ K}$. Figure 3(b) summarizes the τ_r of the fast component for the as-grown sample and that annealed at 650 °C. The τ_r for the sample annealed at 650 °C clearly increases with the temperature at above 20 K. The linear increase in the τ_r results from the spectral linewidth extension with acoustic-phonon scattering.^{27,28} Therefore, the linear increase of 38 ps/K in the τ_r for the sample annealed at 650 °C indicates that the 2D energy dispersion is formed in the epitaxial N δ -doped layer by the RTA process.

To investigate the 2D property of the epitaxial N δ -doped layer, we performed magnetic-field-dependent PL measurements. Figures 4(a) and 4(b) summarize the magnetic field dependence of the PL spectra for the as-grown sample and that annealed at 650 °C, respectively. The excitation power density was 25 W/cm². The magnetic field intensity was increased up to 5 T in the Faraday configuration. Figure 4(c) shows the magnetic field dependence of the PL

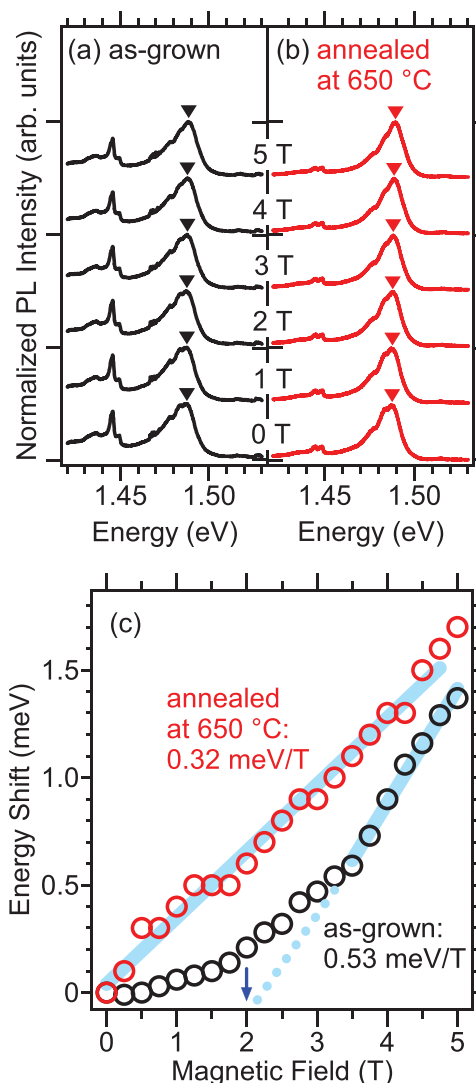


FIG. 4. Magnetic field dependence of the PL spectra for (a) the as-grown sample and (b) the sample annealed at 650 °C at 4.3 K. PL spectra were normalized at the 1.47–1.49 eV band. (c) Magnetic field dependence of the PL-peak energy of the as-grown sample and that annealed at 650 °C. The solid lines show the fitting results.

peak energy indicated by triangles in Figs. 4(a) and 4(b). Here, the minimal PL peak energy was set to zero. In both cases, the PL peak energies exhibited blueshifts by increasing the magnetic field intensity. For the as-grown sample, the PL peak energy exhibited a quadratic shift below the field intensity of 3 T, which indicates that electronic states are localized in the N δ -doped layer in GaAs.¹³ Conversely, a clear linear shift appeared above the field intensity of 3.5 T. This so-called ‘Landau shift’ represents magnetic quantization of the delocalized energy states and is attributed to the cyclotron motion in the growth plane.¹³ This Landau shift signals the 2D delocalization of the electronic states in the N δ -doped layer. On the other hand, for the sample annealed at 650 °C, the PL peak energy exhibited the Landau shift obviously starting from ~ 0 T, implying that the electronic states in this case are perfectly delocalized in the (001) plane. The increase in the number of fourth-nearest-neighbor N pairs implies the homogenization of these N pairs, and the reduction in the number of non-radiative recombination centers implies the reduction in the number of electron traps obstructing the cyclotron motion. It has been reported that N atoms slightly diffuse along the growth direction by a RTA at 900 °C in Ga(As,N)/GaAs MQWs according to transmission electron microscopy analysis,²⁹ suggesting that the RTA for our N δ -doped layer also may cause N-pair configurations distributing along the growth direction. However, the obvious Landau shift demonstrates that the 2D nature of the N δ -doped layer in the (001) plane is remarkably enhanced by the RTA.

From the Landau shift energy, $\Delta E = (e\hbar/2\mu)B$, the in-plane reduced effective mass of the exciton, μ , was estimated as $0.11m_0$ and $0.18m_0$ for the as-grown sample and that annealed at 650 °C, respectively. Here, m_0 is the electron rest mass. The cyclotron angular frequency ω_c is eB/μ , and the Landau shift is observed for $\omega_c\tau_c > 1$, where τ_c is the carrier relaxation time. Consequently, the lower limit on the carrier relaxation time is provided by μ/eB . The Landau shift was observed starting from ~ 0 T for the sample annealed at 650 °C, which resulted in a drastic increase in the carrier relaxation time τ_c and mobility $e\tau_c/\mu$. The calculated lower limits on the carrier relaxation time and mobility were approximately 4 ps and $40\,000\text{ cm}^2/\text{V s}$ for the sample annealed at 650 °C for the field intensity of 0.25 T (corresponding to the lowest magnetic field intensity in this study). Conversely, for the as-grown sample for the field intensity of 2.0 T, the corresponding values were approximately 0.3 ps and $5000\text{ cm}^2/\text{V s}$. Here, the critical magnetic field intensity of 2.0 T was estimated from the intercept of the linear magnetic-field dependence of the PL peak energy as shown by the arrow in Fig. 4(c). According to these results, the carrier mobility for the sample annealed at 650 °C is at least one order of magnitude higher than that for the as-grown sample.

In conclusion, we investigated the effects of RTA in the epitaxial N δ -doped layer in GaAs. We found that RTA caused a rearrangement of the N atoms from the

first-nearest-neighbor N pairs to the fourth-nearest-neighbor N pairs, reducing the number of non-radiative recombination centers. Furthermore, a linear increase in the radiative lifetime with the temperature demonstrated the 2D energy dispersion formation in the epitaxial N δ -doped layer by the RTA. Thereby, a Landau shift was observed at around zero magnetic field intensity, demonstrating a dramatic increase in the carrier mobility if the scattering processes are ignored. These results show that 2D delocalized electronic states in the (001) plane can be achieved by rearranging the N atoms.

- ¹D. Bimberg and U. W. Pohl, *Mater. Today* **14**, 388 (2011).
- ²M. Bayer, P. Hawrylak, K. Hinzer, S. Fafard, M. Korkusinski, Z. R. Wasilewski, O. Stern, and A. Forchel, *Science* **291**, 451 (2001).
- ³E. A. Stinaff, M. Scheibner, A. S. Bracker, I. V. Ponomarev, V. L. Korenev, M. E. Ware, M. F. Doty, T. L. Reinecke, and D. Gammon, *Science* **311**, 636 (2006).
- ⁴L. Wang, A. Rastelli, S. Kiravittaya, M. Benyoucef, and O. G. Schmidt, *Adv. Mater.* **21**, 2601 (2009).
- ⁵D. Alonso-Álvarez, J. M. Ripalda, B. Alén, J. M. Llorens, A. Rivera, and F. Briones, *Adv. Mater.* **23**, 5256 (2011).
- ⁶A. Takahashi, T. Ueda, Y. Bessho, Y. Harada, T. Kita, E. Taguchi, and H. Yasuda, *Phys. Rev. B* **87**, 235323 (2013).
- ⁷P. M. Koenraad and M. E. Flatté, *Nat. Mater.* **10**, 91 (2011).
- ⁸Y. Harada, M. Yamamoto, T. Baba, and T. Kita, *Appl. Phys. Lett.* **104**, 041907 (2014).
- ⁹T. Kita and O. Wada, *Phys. Rev. B* **74**, 035213 (2006).
- ¹⁰T. Kita, Y. Harada, and O. Wada, *Phys. Rev. B* **77**, 193102 (2008).
- ¹¹Y. Harada, T. Kubo, T. Inoue, O. Kojima, and T. Kita, *J. Appl. Phys.* **110**, 083522 (2011).
- ¹²F. Ishikawa, S. Furuse, K. Sumiya, A. Kinoshita, and M. Morifuji, *J. Appl. Phys.* **111**, 053512 (2012).
- ¹³T. Mano, M. Jo, K. Mitsuishi, M. Elborg, Y. Sugimoto, T. Noda, Y. Sakuma, and K. Sakoda, *Appl. Phys. Express* **4**, 125001 (2011).
- ¹⁴T. Makimoto, H. Saito, T. Nishida, and N. Kobayashi, *Appl. Phys. Lett.* **70**, 2984 (1997).
- ¹⁵W. Okubo, S. Yagi, Y. Hijikata, K. Onabe, and H. Yaguchi, *Phys. Status Solidi A* **211**, 752 (2014).
- ¹⁶S. Francoeur, J. F. Klem, and A. Mascarenhas, *Phys. Rev. Lett.* **93**, 067403 (2004).
- ¹⁷W. K. Cheah, W. J. Fan, S. F. Yoon, W. K. Loke, R. Liu, and A. T. S. Wee, *J. Appl. Phys.* **99**, 104908 (2006).
- ¹⁸S. Shirakata, M. Kondow, and T. Kitatani, *Appl. Phys. Lett.* **80**, 2087 (2002).
- ¹⁹R. C. Plantenga, V. R. Kortan, T. Kaizu, Y. Harada, T. Kita, M. E. Flatté, and P. M. Koenraad (unpublished).
- ²⁰D. Sentosa, X. Tang, Z. Yin, and S. J. Chua, *J. Cryst. Growth* **307**, 229 (2007).
- ²¹W. K. Loke, S. F. Yoon, S. Z. Wang, T. K. Ng, and W. J. Fan, *J. Appl. Phys.* **91**, 4900 (2002).
- ²²E. Tournié, M.-A. Pinault, and A. Guzmán, *Appl. Phys. Lett.* **80**, 4148 (2002).
- ²³M. Ramsteiner, D. S. Jiang, J. S. Harris, and K. H. Ploog, *Appl. Phys. Lett.* **84**, 1859 (2004).
- ²⁴J.-M. Chauveau, A. Trampert, K. H. Ploog, and E. Tournié, *Appl. Phys. Lett.* **84**, 2503 (2004).
- ²⁵Y. Harada, O. Kojima, T. Kita, and O. Wada, *Phys. Status Solidi B* **248**, 464 (2011).
- ²⁶P. Lefebvre, J. Allègre, B. Gil, A. Kavokine, H. Mathieu, W. Kim, A. Salvador, A. Botchkarev, and H. Morkoç, *Phys. Rev. B* **57**, R9447 (1998).
- ²⁷J. Feldmann, G. Peter, E. O. Göbel, P. Dawson, K. Moore, C. Foxon, and R. J. Elliott, *Phys. Rev. Lett.* **59**, 2337 (1987).
- ²⁸L. Schultheis, A. Honold, J. Kuhl, K. Köhler, and C. W. Tu, *Phys. Rev. B* **34**, 9027(R) (1986).
- ²⁹G. Mussler, J.-M. Chauveau, A. Trampert, M. Ramsteiner, L. Däweritz, and K. H. Ploog, *J. Cryst. Growth* **267**, 60 (2004).